Article

Not peer-reviewed version

Determination of Combustion Experimental Conditions of Different Pellets Based on Ostwald Diagrams in a Domestic Boiler

Juan Félix González , Andrés Álvarez Murillo , Diego Díaz García , Sergio Nogales-Delgado *

Posted Date: 28 September 2023

doi: 10.20944/preprints202309.1974.v1

Keywords: combustion; biomass; optimization; biomass; pine; poplar; plum tree; fume analysis.

Preprints (www.preprints.org) | NOT PEER-REVIEWED | Posted: 28 September 2023 doi:10.20944/preprints202309.1974.v1

Article

Determination of Combustion Experimental Conditions of Different Pellets Based on Ostwald Diagrams in a Domestic Boiler

Juan Félix González [1], Andrés Álvarez Murillo [2], Diego Díaz García [1] and Sergio Nogales-Delgado [1,*]

[1] Department of Applied Physics, University of Extremadura. Avda. De Elvas, s/n, 06006, Badajoz (Spain).
[2] Department of Teaching of Experimental Sciences and Mathematics, Avda. De Elvas s/n, 06006, Badajoz (Spain).
* Correspondence: senogalesd@unex.es

Featured Application: A thorough study about the optimization of a real biomass stove by using different fuels was carried out to determine the quality of exhaust gases.

Abstract: Global energy scenario is becoming vital for the sustainable economic development of a region or country. Current changes in energy production, mainly due to scarcity and geopolitical factors, have proven the need for changes in energy mix towards a lower energy dependence. In that sense, a considerable amount of biomass waste is generated in many regions, because of agro-industrial activities, whose management could contribute to energy production. The aim of this work was to study the determination of combustion conditions in a biomass stove by using different raw materials as fuels, such as pine, poplar, and plum tree pellets. For that purpose, power, excess air, and biomass content were optimized, among other parameters, and fumes were analyzed with a Testo 335 analyzer, recording temperatures with temperature probes. As a conclusion, high yields were found for the optimized parameters of the studied biomass (ranging from 91.1 % for poplar pellet to 92.34 % for pine pellet), making these three biomass fuels suitable for combustion in the abovementioned stove. Also, increasing biomass flow by 25 % in the stove contributed to a higher efficiency of the process, especially in the case of plum tree pellets.

Keywords: combustion; biomass; optimization; biomass; pine; poplar; plum tree; fume analysis

1. Introduction

1.1. Global Energy Scenario

Global energy scenario is one of the most challenging issues when it comes to the global development of a country. Current oscillations in energy production due to many factors such as geopolitics or international relations have pointed out, in the case of many countries (especially smaller or less-powerful ones, which are usually more dependent and vulnerable compared to world powers such as China or USA [1]), the need for modifications in energy patterns towards less energy dependency, which would imply a boost for their economies and industrial activities [2], possibly reducing the influence of international oil companies (IOCs) in energy transition, as in the case of Europe [3]. In that sense, the possibility for many countries to become "prosumer actors" through a green transition could reduce any form of geopolitical concern [4]. For instance, in the case of Europe (according to recent studies), it is vital to replace energy imports with domestic energy production, reducing energy dependency. If import substitution takes place with domestic renewable energy sources, additional positives effects could be found in terms of energy dependency and security and sustainable development [5]

 doi:10.20944/preprints202309.1974.v1

Additionally, there is an increasing concern (at national and international level) about environmental issues such as climate change, with greenhouse gas emissions being one of the most worrying aspects related to industrial activities and energy consumption. This way, international organizations such as the United Nations have been fostering the Sustainable Development Goals (SDG), where the implementation of specific steps to promote the sustainable economic and energy growth (especially in the case of developing countries) have an essential role, promoting concepts such as green chemistry, circular economy or atom efficiency, among others, in order to maintain the environmental quality of soil, water and air [6].

Specifically, the use of biomass could play an important role in the implementation of these SDGs or similar biomass, bioprocessing or biobased product policies, implying in many cases the valorization of wastes with a difficult environmental management through its energy use at local and industrial levels, possibly contributing to bioeconomy strategies (which many of them are not still completely coherent with common bioeconomy objectives), being an interesting resource to improve the use of marginal lands that can alleviate resource competition and soil deterioration [7].

In that sense, some data included in Figure 1 supports the abovementioned reasoning. Thus, if worldwide pellet production is considered (Figure 1a), an exponential increase can be observed in the last two decades, which points out the commercialization of biomass at a global level. Also, in the case of Europe (Figure 1b), there was a steady increase in solid biomass primary energy production, from around 50 million tons of oil equivalent in 2000 to about 100 million tons in 2021 (that is, doubling the production). This fact could imply an increase in the implementation of biomass power plants. For instance, regarding Germany (Figure 1c) there was a 16 % increase in biomass power plants in the last decade, pointing out the commitment of this country with renewable energies, including biomass. Last but not least, the role of biomass in some developing regions or countries could be important, as shown in Figure 1d for electricity generation from biomass and waste in Africa. As observed, the electricity generation doubled in two decades, considering this energy source as an interesting way to contribute, among other renewable energies, to the sustainable development of Africa. Indeed, interesting works have been carried out about the use of local biomass in boilers, as in the case of Cameroon [8].

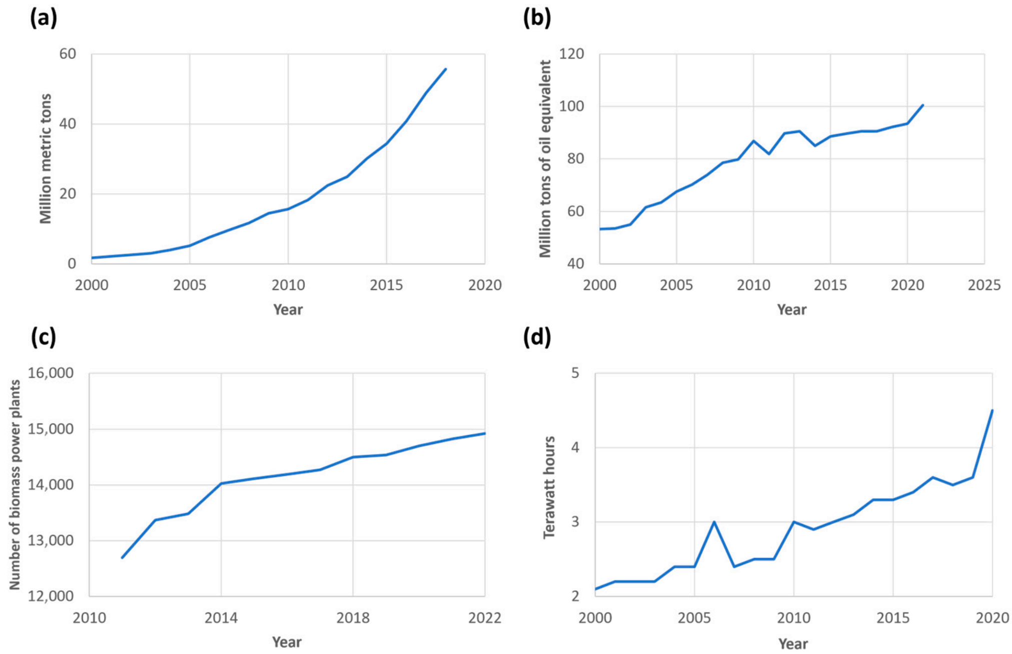

Figure 1. Different trends regarding biomass in the last two decades: a) Global wood pellet production (source: [9]); b) Solid biomass primary energy production in Europe (source: [10]); c) Number of biomass power plants in Germany (source: [11]); d) Electricity generation (in terawatt hours) from biomass and waste in Africa (source: [12]).

 doi:10.20944/preprints202309.1974.v1

These data support the contribution of this energy source to the sustainable development in general, increasing the energy independence of countries and regions and managing some agricultural wastes, improving their valorization. In general, biomass energy use is devoted for a local consumption, that is, many countries such as Finland or Sweden consume almost all biomass energy produced by themselves [13,14]. Nevertheless, there are other countries where biomass energy production exceeds its consumption, as in the case of Portugal [15], whereas the opposite also takes place, with a higher consumption compared to biomass energy production (for instance, in Italy) [16]. In any case, these differences are not noticeable, showing relatively similar biomass energy production and consumption.

Concerning Spain (whose biomass energy production/consumption is also balanced, according to recent data [17]), and specifically in Extremadura region, a considerable amount of biomass wastes is continuously generated due to diverse agro-industrial activities. Nevertheless, these wastes present a high potential for energy generation (including barks, husks, corncob, etc.), which represents a great opportunity for the implementation of circular economy or green chemistry policies [18,19]. Conventionally, these wastes are used for direct combustion and the subsequent energy generation through steam cycles. In that sense, combustion optimization (for instance, taking place in a stove) is essential to make this process energy and economically feasible at user and industrial levels.

1.2. Combustion: Foundations and Optimization

Combustion is a chemical reaction where an oxidizing air is combined with oxidable elements included in a combustible substance. This chemical reaction energy is released as heat. The obtained chemical species are considered reaction products, exhausted gas, or combustion gas. For this purpose, pure oxygen is not usually used, whereas oxidizing gas is normally employed (for instance, air). Thus, there are different kinds of combustion, such as complete combustion (where the combustible is completely oxidized), neutral combustion (a complete combustion where stoichiometric oxygen is used) and incomplete combustion (where the combustible is not completely oxidized).

In that sense, heating value of a fuel is the heat released in a complete combustion for a unit of fuel. This way, heating value can be determined as high heating value (HHV) and low heating value (LHV), depending on the consideration of steam condensation due to combustion or water content in fuel. Thus, the only difference between HHV and LHV is the condensation heat of steam (produced during combustion or included in fuel). Therefore, this parameter is extremely important in this context, as the use of fuels with a specific heating value will determine the efficiency of combustion processes in stoves.

Combustion facilities, such as those including stoves, are usually designed to obtain the highest yield, that is, an optimum yield, in order to make combustion as much efficient as possible. For that purpose, energy loss should be minimal. Thus, loss due to sensible heat or solid and gaseous non-burnt products can be reduced if the excess air coefficient (n, included in Equation 1) is adjusted, which is difficult to find in a specific facility.

$$n = \frac{air_r}{air_t} \qquad (1)$$

Where air_r is the real air in the facility and air_t is the theoretical air that should be provided. Thus, loss due to sensible heat is due to the fact that a percentage of the generated heat during combustion is not useful, as the exhausted gas are evolved at higher temperatures compared to ambient temperature. Considering the exhausted fumes (P_s) as a mixture of ideal gases, this loss can be assessed according to Equation 2:

$$P_s = \Delta H = h_h - h_a = m_h C_{ph}(T_h - T_a) = V_h \rho_h C_{ph}(T_h - T_a) \qquad (2)$$

Where:

- $h_h - h_a$ represents the enthalpy change in exhausted fumes.
- m_h is the exhausted flow.
- C_{ph} is the average specific heat of fumes.
- $T_h - T_a$ is the inlet and outlet temperature (respectively) of fumes and air.
- V_h and ϱ_h are total volume generated and fume density, respectively.

Preprints (www.preprints.org) | NOT PEER-REVIEWED | Posted: 28 September 2023 doi:10.20944/preprints202309.1974.v1

Thus, loss could be avoided if $V_h = 0$ or $T_h = T_a$. The way to reduce these losses is to decrease outlet temperature and total volume of fumes. In the first case, heat recovery systems are used for fumes to decrease T_h, air heaters to increase T_a. Also, superheaters or reheaters can be used for this purpose. Regarding total fume volume reduction, it can be achieved by reducing excess air. In fact, this loss is minimal if minimum air necessary for combustion of a specific combustible is used.

Loss due to non-combusted gas are on account of the presence of combustible gas, mainly CO. Low heating value (LHV) in a solid fuel can be calculated, according to its elemental analysis, through Equation 3:

$$LHV = 8100P_C + 34400P'_{H_2} + 2500P_S + 5400P_{H_2} \quad (3)$$

Where P_C is the percentage in weight of carbon obtained in ultimate analysis, P_{H2} is the percentage in weight of hydrogen obtained in ultimate analysis and P_S is the percentage in weight of sulfur obtained in ultimate analysis, all of them expressed in kg of each element per kg of fuel. If total combustion of carbon takes place, the following reaction occurs (see Equation 4):

$$C + O_2 \rightarrow CO_2 + 8100\ kcal/kg \quad (4)$$

If combustion is incomplete (obtaining CO), P_C value would be P_C·(1-x), and the following reaction takes place (Equation 5):

$$C + \frac{1}{2}O_2 \rightarrow CO + 2430\ kcal/kg \quad (5)$$

Where x is the burned gas ratio, (1-x) is the unburned gas ratio (which is evolved), $P'_{H2} = P_{H2} - P_{O2}/8$ (for wet basis) and $P'_{H2} = P_{H2}$ for dry basis. Thus, according to Equation 6:

$$x = \frac{v_{CO_2}}{v_{CO} + v_{CO_2}} \quad (6)$$

The loss due to unburned gas (P_{ub}) would be obtained according to Equation 7:

$$P_{ub}(CO) = 8100P_C - [8100P_C x + 2430\ P_C\ (1-x)] = 5670P_C(1-x) \quad (7)$$

Where P_C is the amount of carbon in biomass. From the previous equation it can be inferred that the lower the value of x, that is, the more incomplete combustion, the higher the loss will be found. Therefore, this loss will be avoided carrying out a complete combustion. This can be achieved by pulverizing the fuel, provoking turbulences to increase the contact between the oxidizing agent and the fuel, providing a suitable excess air coefficient, increasing the heat at homes, or increasing the residence time.

Therefore, concerning these losses, an optimum excess air coefficient is needed to contribute to a maximum yield, as observed in Figure 2. The indirect method to determine the yield of the process is based on the calculation of all losses that takes place in the oven through Equation 8:

$$\eta = 1 - \frac{\sum P}{LHV} \quad (8)$$

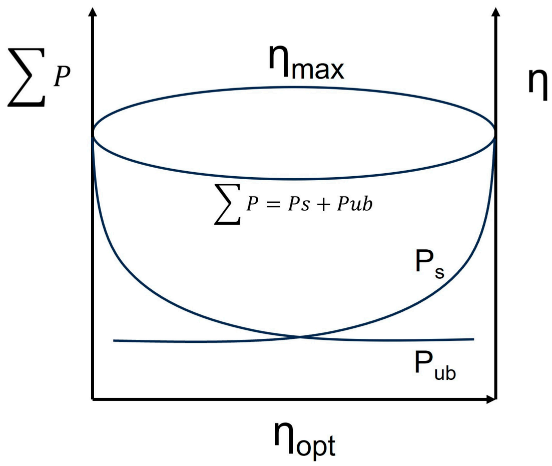

Figure 2. Loss, yield, and excess air coefficient.

The graphical representation of loss through sensitive and latent enthalpy presents a disadvantage, that is, the impossibility of finding a general mathematical expression that correlates both losses according to excess air (n). For this reason, the only reliable way to represent these

Preprints (www.preprints.org) | NOT PEER-REVIEWED | Posted: 28 September 2023 doi:10.20944/preprints202309.1974.v1

equations is through experimental sampling for each combustion facility, testing different excess air ratios.

1.3. Ostwald Diagram: Theoretical Foundations

In order to optimize combustion processes, a mathematical tool (developed by Wilhelm Ostwald and used in the literature for some time to determine the performance of biomass facilities [20]) is going to be used from the fuel parameters obtained for each combustion stage. If fume composition is known in percentage, it is possible to represent the stage of the process. According to Figure 3, an example of an Ostwald diagram can be observed.

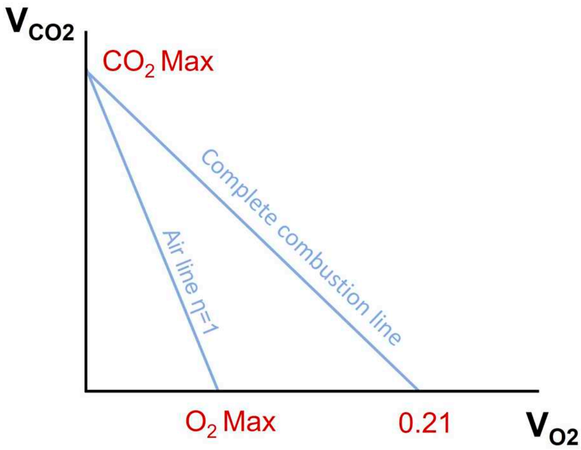

Figure 3. Example of an Ostwald diagram.

Thus, the two cathetus or legs represent the values of V_{CO2} and V_{O2} in fumes, and the hypotenuse represents the complete combustion line. The triangle is divided, in turn, by the so-called air line, in two parts: one representing the incomplete combustion points due to the lack of air (triangle corresponding to the ordinate-abscissa-air lines) and another one representing the incomplete combustion due to excess air (triangle corresponding to the air-abscissa-complete combustion lines).

Regarding the complete combustion line, it is the geometric line corresponding to V_{CO2} and V_{O2}, that is, corresponding to complete combustion (see Equation 9).

$$V_{O_2} + V_{CO_2}\left(1 + 0.79\frac{3P'_{H_2}}{P_C}\right) = 0.21 \qquad (9)$$

This way, this line has a value at the abscissa axis of 0.21, whereas its value at the ordinate axis is CO_2 max. This first point, CO_2 max, V_{O2} = 0 (which corresponds to a combustion in the absence of oxygen, that is, a neutral combustion with n=1), depends on the kind of fuel (its composition), whereas the value at the abscissa axis is 0.21 regardless the fuel used and, therefore, it is common to every Ostwald diagram. Concerning air line, it is the line whose excess air coefficient equals one. For its representation, previous equations are required. If n=1 and CO_2 max and O_2 max are calculated, the intersection points with the abscissa and ordinate axis are obtained (Equations 10 and 11):

$$V_{CO_2} = \frac{\frac{P_C}{12}x}{\frac{100n-21}{21}\left(\frac{P_C}{12}+\frac{P'_{H_2}}{4}\right)+\frac{P_C\left(1+\frac{1-x}{2}\right)}{12}} \qquad (10)$$

$$V_{O_2} = \frac{\left(\frac{P_C}{12}+\frac{P'_{H_2}}{4}\right)(\eta-1)+\frac{1}{2}\frac{P_C}{12}(1-x)}{\frac{100n-21}{21}\left(\frac{P_C}{12}+\frac{P'_{H_2}}{4}\right)+\frac{P_C\left(1+\frac{1-x}{2}\right)}{12}} \qquad (11)$$

Line n=1 divides the triangle in two parts, the one on the left corresponding to incomplete combustion due to the lack of air and the one on the right corresponding to incomplete combustion due to excess air. It should be noted another property of line n=1, as $V_{CO} = 2V_{O2}$, if V_{O2} values are correlated to this line, V_{CO} scale is obtained by multiplying these values by two, which is a scale that can be projected over an additional axis, perpendicular to the hypotenuse of the triangle. Regarding the lines obtained when V_{CO} is constant, even though these are theoretical curves, they can be

Preprints (www.preprints.org) | NOT PEER-REVIEWED | Posted: 28 September 2023 doi:10.20944/preprints202309.1974.v1

considered straight lines, as the difference is negligible. Thus, these lines are obtained by drawing parallel lines to the hypothenuse. When giving other values to n and replacing in the previous equations, the lines when n is constant are obtained.

1.4. Novelty and Aim of This Work

As explained, the role of a combustion is vital to increase the efficiency of domestic or industrial stoves and, subsequently, the sustainability of the process, reducing the amount of pollutants evolved to the atmosphere depending on factors such as biomass composition [21,22], previous conditions [23], stove design (including its evolution to improve performance) [24–26] or burning conditions [27–29]. Thus, some works dealt with this subject, as observed in Table 1. These works are focused on evolved pollutants applied to the use of domestic, industrial stoves or simulations [30], focused on variables such as the kind of biomass, biomass load or pre-treatments like wood washing or drying [31].

Table 1. Recent works related with the subject of this research.

Authors	Details and findings	Reference
Maxwell et al.	Analysis of the emissions of three different biomass and their torrefied counterparts in a domestic wood stove. After torrefaction, lower emissions (CO and CH_4) were found.	[32]
Prapas et al.	Study of the influence of a chimney on the combustion characteristics of a stove, observing changes in CO production.	[33]
Sungur et al.	Optimization of the effect of burner pot design by changing supply airflow position in a pellet stove through machine learning.	[34]
Schmidt et al.	Influence of wood washing on emissions during wood combustion in a domestic pellet stove, with a decrease in pollutants.	[35]
Vicente et al.	Wood combustion experiments were carried out to determine the effect of different factors like biomass load.	[36]
Toscano et al.	Combustion tests were carried out simulating domestic utilization conditions of a pellet stove. Higher emissions (for instance, CO) were found in steady state condition.	[37]

In that sense, the novelty of this work consists in the optimization of a pellet stove considering both raw materials and parameters depending on the stove like power (which depends on the working level or position of the stove). Thus, an adapted optimization of a specific stove for each kind of biomass is offered, assessing the influence of raw material on combustion optimization.

Considering the above, in more detail, the aim of this work was to carry out the optimization of the combustion process in a commercial stove. For that purpose, different kinds of fuels were used at different air ratios and levels or positions, assessing efficiency according to fume flow and composition.

2. Materials and Methods

2.1. Facilities, Raw Materials and Their Characterization

This work was carried out in the Department of Applied Physics, belonging to the Engineering School at the University of Extremadura, consisting of the optimization study of a biomass combustion stove, using a commercial biomass stove and working at 10 Pa and 5 kW, operating with different fuels such as pine, poplar, and plum tree pellets provided by CICYTEX (Centro de Investigaciones Científicas y Tecnológicas de Extremadura). Thus, through experimental studies, the performance of this stove was optimized according to the raw material, feeding ratio and power.

The samples were collected and homogenized to avoid considerable statistical errors due to heterogeneity, preparing 1-2 g of sample for each characterization. Thus, the following determinations were carried out, which were summarized in Table 2:

Table 2. Raw material characterization, including details according to the international standards.

Parameter	Details
Proximate analysis	It consists of biomass composition regarding ash, moisture, volatile content, and fixed carbon.
Ash content	It is the solid waste after incineration. High-quality fuels present low ash content. Determination according to UNE 32004:1984 standard [38]
Moisture content	High moisture reduces energy potential as some energy will be used to evaporate and remove moisture. According to UNE 32001:1981 standard [39]
Volatile matter	Weight loss of a fuel during heating in absence of oxygen (apart from moisture content). According to UNE 32019:1984 standard [40]
Fixed carbon	It is obtained according to the previous values, as follows: Fixed carbon = 100 – (% ash + % moisture + % volatile matter).
Ultimate analysis	It is the qualitative and quantitative determination of certain chemical elements such as C, H, N, S and O, mainly.

2.2. Combustion System and Equipment

The main components of the combustion process were the following (see Figures 4 and 5):

- Pellet stove, where the different biomass pellets were fed to carry out their combustion at different feed ratios and power.
- Gas analyzer for combustion fumes (Testo 335), placed in the chimney once to analyze the main components included in combustion fumes such as O_2, CO_2 or CO.
- Temperature probe for fumes.
- Temperature probe for inlet air.

Regarding the pellet stove (Isabella), it presented the following characteristics (included in Table 3):

Table 3. Main characteristics of the combustion stove.

Parameter	Result
Weight, kg	110
Height, mm	864
Width, mm	453
Depth, mm	497
Fume pipe diameter, mm	80
Air suction pipe diameter, mm	50
Maximum heating volume, m^3	115
Maximum thermal power, kW	5.8
Maximum useful thermal power, kW	5.0
Minimum useful thermal power, kW	2.5
Maximum hourly fuel consumption, kg/h	1.2
Minimum hourly fuel consumption, kg/h	0.6
Tank capacity, kg	11
Nominal electric power, W	300
Recommended flue gas pressure, Pa	10
Flue gas pressure at maximum thermal power, Pa	12

Flue gas pressure at minimum thermal power, Pa	10

Thus, Figures 4a and b show the abovementioned stove. Regarding the gas analyzer (Testo 335, Figure 4c), it is a portable analyzer specifically used for combustion gas analysis, measuring room temperature and outlet temperature (°C), oxygen (%), NO (ppm) and CO (ppm), and calculating some parameters from these data such as excess air coefficient (n), thermal yield (η) and loss through sensitive enthalpy in fumes (q_a). The temperature probe for exhaust fumes (Figure 4d) is connected to a digital display, indicating temperature values in °C. Finally, temperature probe for inlet gas (Figure 4e) is equally connected to a digital display, expressing temperature in °C.

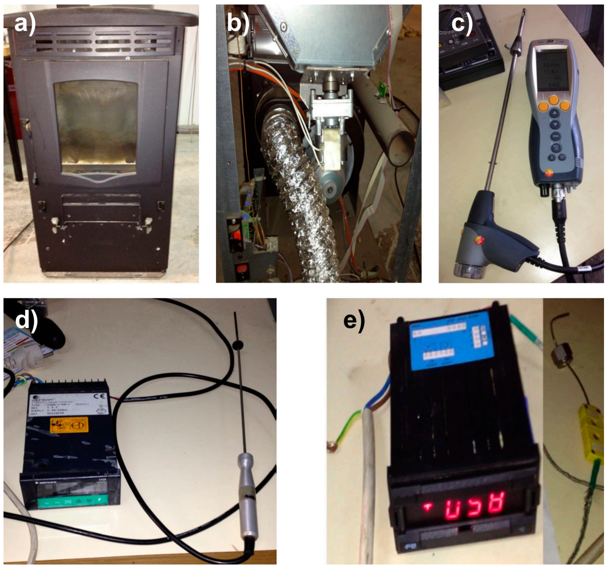

Figure 4. Main components of the biomass stove, including: a) stove (front view) ; b) stove (back view) c) gas analyzer (Testo 335); d) temperature probe for exhaust fumes; e) temperature probe for air supply.

Finally, Figure 5 shows the arrangement of the abovementioned components in the experimental facility, which serves as a guide for the experimental procedure explained in the following subsection. Thus, as recommended in the literature, sampling of these kind of pollutants (CO, CO_2, NO_x, etc.) is usually carried out by gaseous analyzers placed in the chimney, after combustion took place [41].

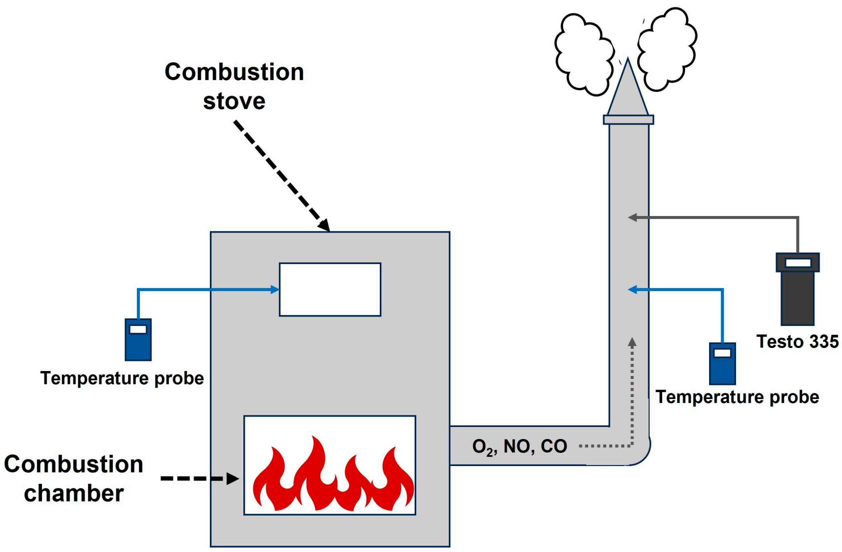

Figure 5. Scheme of the combustion system.

doi:10.20944/preprints202309.1974.v1

2.3. Experimental Procedure

In this subsection, the main steps carried out during combustion are be explained, which are the main step to obtain the Ostwald diagram (an essential tool to assess the results obtained in this combustion chamber) according to experimental data.

First, the fuel hopper is filled with the corresponding biomass (pine, poplar, or plum tree pellets). Afterwards, the stove is switched on, and the primary fan started working. After 2 minutes, the worm screw started feeding the combustion chamber with pellets, and once the ignition started, combustion took place. It should be noted that the stove needed a constant pellet feed to avoid an automatic shutdown. Once the flame is generated in biomass, the stove started to work, and the secondary fan started working after 2 minutes, starting the heat release from the front part of the combustion stove. The feeding rate and fan power are increased from Position 1 to Position 5, which are the five working levels of the stove. Also, for each working level or position, a normal pellet feed (100 %) can be carried out, increasing this value 25 % considered "Extra feed". The steady state will be achieved after 90 minutes depending on the position or level selected, and then another test can be carried out by changing the kind of pellet, for instance. The measurements taken by the Testo analyzer were carried out placing the probe in the fume pipe (see Figure 5). The different conditions selected for pellet combustion are included in Table 4, where different raw materials, levels and feed ratios were used to assess their effect on combustion stove performance. As observed in this table, five different levels can be used in this stove, with an increasing feeding rate and primary fan power. A selection of these combustion conditions will be discussed in Results and Discussion section.

Table 4. Main conditions selected for pellet combustion.

Raw material	Position or level selected	Pellet feed
Pine Poplar Plum tree	1, 2, 3, 4 and 5	Normal (100 %) Extra (125 %)

2.4. Ostwald Diagram

In this section, the calculation of the Ostwald diagram is shown in detail (giving as an example the case of poplar pellet combustion, with the rest of fuels showing an equivalent behavior), as a complementary tool apart from the equipment used for the combustion system. Thus, the complete combustion line, as well as air line (n=1), air lines at different n values (1.5, 2, etc.) and the lines at constant CO values are explained.

Regarding the complete combustion line, Table 5 shows the points obtained in the case of poplar pellet combustion. As observed, V_{CO2} values are obtained from Equation 9. The slope determination of complete combustion line (m_{ccl}) is obtained by using a line passing through two selected points (X_1, Y_1) and (X_2, Y_2). For that purpose, a and b parameters are determined, where a is the slope of the line and b is the independent term (see Equations 12 and 13).

Table 5. Points of complete combustion line for poplar pellets.

V_{O2}, % (X)	V_{CO2}, % (Y)	V_{O2}, % (X)	V_{CO2}, % (Y)
0.00	0.161	0.11	0.077
0.01	0.153	0.12	0.069
0.02	0.145	0.13	0.061
0.03	0.138	0.14	0.054
0.04	0.130	0.15	0.046
0.05	0.122	0.16	0.038

0.06	0.115	0.17	0.031
0.07	0.107	0.18	0.023
0.08	0.099	0.19	0.015
0.09	0.092	0.20	0.008
0.10	0.084	0.21	0.000

$$m_{ccl} = a = \frac{Y_1 - Y_2}{X_1 - X_2} \quad (12)$$

$$b = Y_1 - \left(\frac{Y_1 - Y_2}{X_1 - X_2}\right) X_1 \quad (13)$$

In this case, two points from Table 5 are selected: (0.00, 0.16) and (0.21, 0.00), obtaining the corresponding values for m_{ccl} (that is, a) (−0.765) and b (0.1607) according to the abovementioned equations. Figure 6 shows the resulting complete combustion line for poplar pellets.

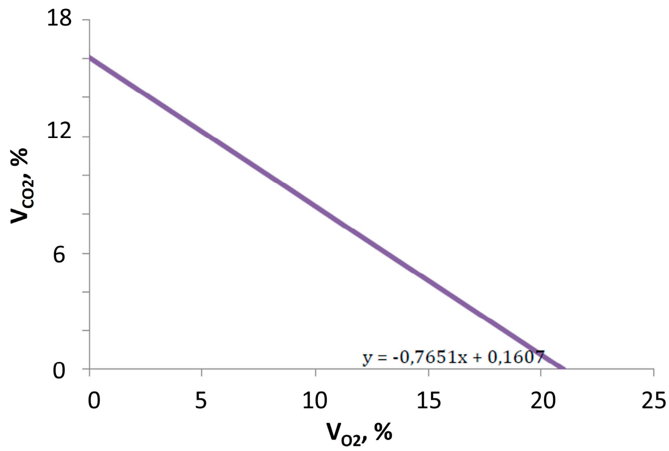

Figure 6. Complete combustion line for poplar.

Regarding air line (n=1), the following equations and points are going to be used: burnt gas ratio (x) is given by Equation 6. The selected points to build air line are the following:

- V_{CO2max}, V_{O2}=0: with n=1 and x=1. $V_{CO2\,max}$ is obtained from Equation 10, obtaining a value of 0.161.
- V_{CO2}=0, V_{O2max}: with n=1 and x=1. $V_{O2\,max}$ is obtained from Equation 11, obtaining a value of 0.074.

From these points (0.000, 0.161) and (0.074, 0.000), the equation of the air line can be obtained, that is, a = −2.16 (in this case, the slope when n=1, $m_{n=1}$) and b = 0.161. The resulting line is shown in Figure 7.

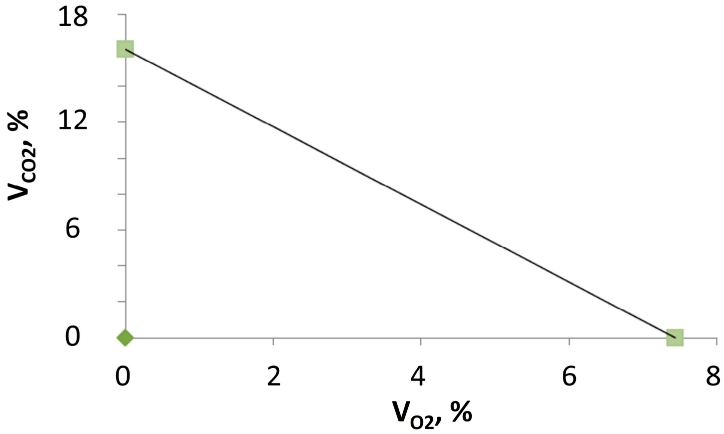

Figure 7. Air line for poplar pellet combustion.

Preprints (www.preprints.org) | NOT PEER-REVIEWED | Posted: 28 September 2023 doi:10.20944/preprints202309.1974.v1

Concerning different values of n (for instance, n = 1.5) for air line, the following elements are going to be used: the slope obtained for air line with n = 1.0 (that is, $m_{n=1}$), the point V_{O2max}, $V_{CO2=0}$ and the following conditions (n = 1.5 and x=0), resulting the following points: (0.119, 0.000) and (0.000, 0.257). Thus, the resulting line is shown in Figure 8:

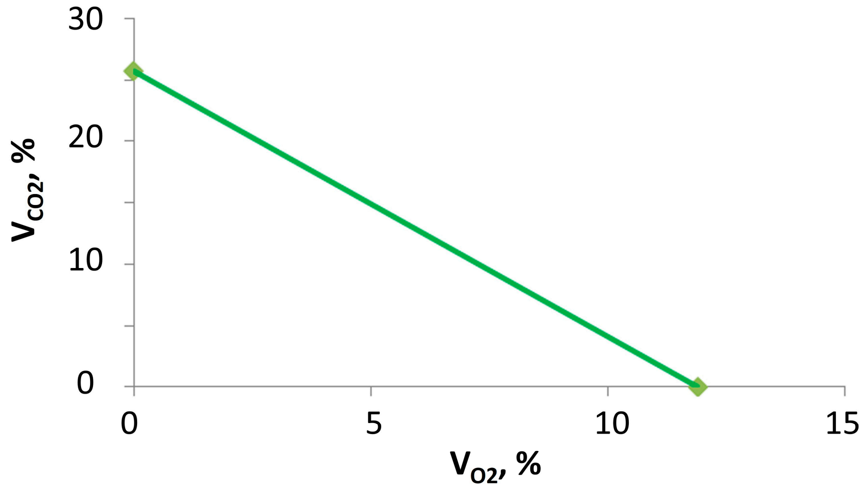

Figure 8. Air line (n=1.5) for poplar pellets.

Concerning constant CO lines, they are obtained when a fixed value of CO was selected. For instance, in the case of CO = 0.02, the intersection point between the air line (n=1) and the line where O_2 is constant is obtained, and then the line given by the abovementioned point and the slope of complete combustion is obtained. Figure 9 shows all the lines obtained at constant values of CO (0.2, 0.4, 0.6, etc.).

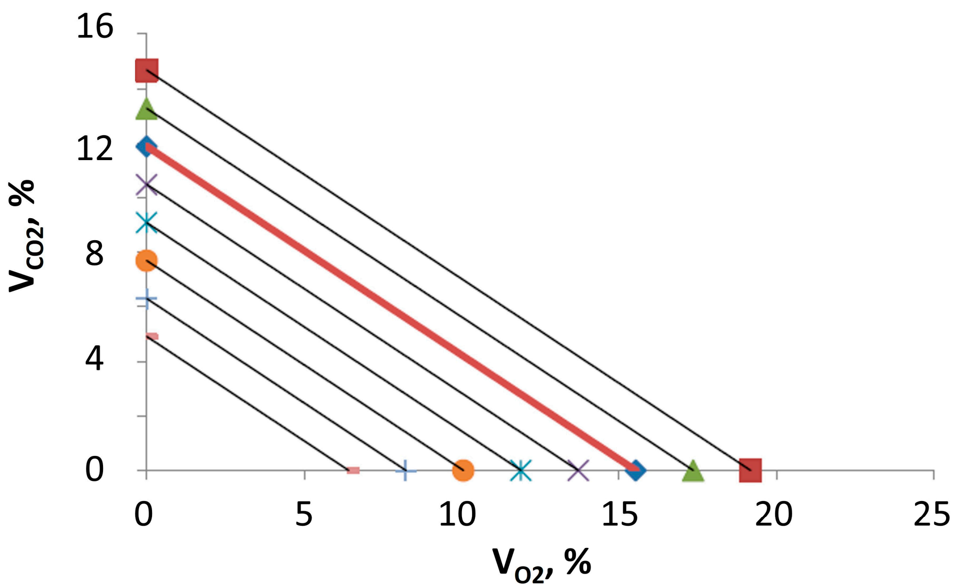

Figure 9. Lines when CO = constant for poplar pellets.

Finally, the Ostwald diagram resulting from the abovementioned calculations in the case of poplar pellet combustion is included in Figure 10.

Preprints (www.preprints.org) | NOT PEER-REVIEWED | Posted: 28 September 2023 doi:10.20944/preprints202309.1974.v1

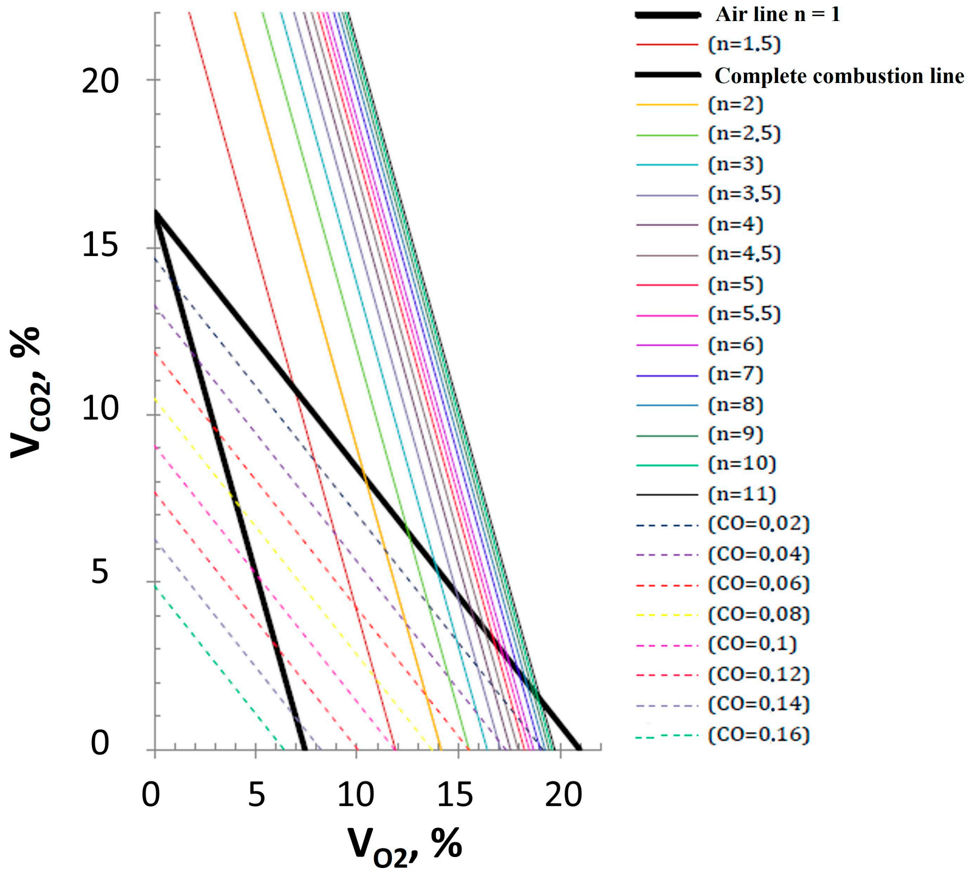

Figure 10. Ostwald diagram for poplar pellets.

This tool will be essential to check the state of the combustion process in the selected stove, in order to assess the optimization of combustion by using different fuels, working levels and pellet feed.

3. Results and Discussion

3.1. Pellet Characterization and Experiments Selected for Combustion Tests

The results found for pine, poplar, and plum tree pellets are included in Table 6:

Table 6. Pellet characterization.

	Proximate analysis				
Sample	Ash, %	Moisture, %	Volatile matter, %	Fixed carbon, %	
Pine	0.50	6.42	84.01	15.49	
Poplar	1.79	6.61	78.24	13.36	
Plum tree	0.83	6.90	78.37	13.90	
	Ultimate analysis				
Sample	C, %	H, %	N, %	S, %	O, %
Pine	47.70	6.12	0.33	0.004	45.85
Poplar	46.40	6.01	0.52	0.028	47.04
Plum tree	47.50	6.23	0.38	0.093	45.80

These results are consistent with other wood pellets found in the literature, whose results were in the same order of magnitude [22,42]. Consequently, it can be concluded that the quality of these pellets, according to proximate and ultimate analysis, is standard compared to the literature. Specifically, it can be seen that the highest ash content was found for poplar pellets, which is within

Preprints (www.preprints.org) | NOT PEER-REVIEWED | Posted: 28 September 2023 doi:10.20944/preprints202309.1974.v1

the normal range found in the literature for pellets obtained from similar species. On the contrary, pine pellets offered the lowest ash content, which is desirable in combustion chambers. HHV for pine, poplar and plum tree pellets were similar, with the following values: 4771, 4714 and 4679 kcal/kg, respectively. Considering that the bulk density of pellets was similar, these results point out that the increase in working level (or positions) included in the stove (from P1 to P5) implies a qualitative increase in power for these experiences.

For each fuel and level included in the stove (from 1 to 5), a test was carried out. Each test included 20 analyses, taking 5 minutes long each, by using the Testo 335 gas analyzer and other two temperature probes. Regarding feeding rate, two different experiments were carried out for each level, with a normal feed (100 %) and 25 % extra feed (125 %). This way, standard biomass will be labeled as "biomass I" and when feeding rate was increased 25 %, "biomass II". As a result, for each experiment with a specific level and feed, the samples were labeled as follows: P (number of level or position) (number of feed). For instance, P2I would correspond to an experiment with the second level at a standard feeding.

For the discussion of results, the tests were compared at the same kind of fuel, as each fuel showed different results regarding proximate and ultimate analysis, and therefore the Ostwald diagram will be different for each case (Table 7). The aim of these comparison was to assess the trends observed for these tests when level and feeding are varied.

Table 7. Levels and feed ratios that are going to be tested for each fuel.

Pine	Poplar	Plum tree
P1I vs P5I	P3I vs P5I	P2I vs P4I
P1I vs P5II	P3I vs P5II	P2I vs P4II
P1II vs P5II	P3II vs P5II	P2II vs P4II
P5I vs P5II	P5I vs P5II	P4I vs P4II

Also, there are some parameters that were theoretically calculated. Thus, the theoretical values, n_{th} (Equation 14), x_{th} (Equation 15) and y_{th} (Equation 16) differed from the ones obtained by the analyzer in the fact that the former consider data of the studied fuel, whereas those obtained by the Testo analyzer are regardless of the kind of fuel. The following equation express the excess air coefficient calculated from data obtained from the tests and data measured by the analyzer for a specific fuel:

$$n_{th} = \frac{-21(-2P_C-6P_H+P_CV_{CO}+6P_HV_{O2}}{(P_C+3P_H)(42+79V_{CO}-200V_{O2})} \quad (14)$$

In the same way, the burned gas ratio is expressed as follows:

$$x_{th} = \frac{-(-42P_C+121P_CV_{CO}+474P_HV_{CO}+200P_CV_{O2}}{P_C(42+79V_{CO}-200V_{O2})} \quad (15)$$

These expressions are determined through the simplification of Equations 11 and 12, used to obtain the air line (n=1). To determine y_{th}, that is, % V_{CO2}, similar steps included in the obtention of lines when CO was constant will be followed. The difference is in point three, where:

$$y = m_{ccl} \cdot \%O_2 + b_s \quad (16)$$

In this case, x will be $\%O_2$ value obtained by the gas meter for a given fuel. Therefore, V_{CO2}, obtained theoretically, will be given by the following expression (Equation 17), which will be used in the tests carried out in this experience.

$$y = V_{CO2} = V_{O2} \cdot m_{Rcc} + m_{n=1}\left(\frac{V_{CO}}{2}\right) + b_{n=1} - m_{Rcc}\left(\frac{V_{CO}}{2}\right) \quad (17)$$

Thus, the results obtained by using these equations are included in following sections.

3.2. Pine Pellet Combustion

Table 8 and Figures 11 and 12 show the main results obtained for pine pellet combustion in our commercial stove when different levels were selected. In Table 8 the extreme levels were compared:

Preprints (www.preprints.org) | NOT PEER-REVIEWED | Posted: 28 September 2023 doi:10.20944/preprints202309.1974.v1

Table 8. Comparison between P1 and P5 for pine pellet combustion.

	P1		P5	
Parameter	**Average**	**Average deviation**	**Average**	**Average deviation**
O_2, %	0.18	0.01	0.148	0.006
Air supply temperature, °C	46.7	1.9	68.4	0.4
Fume temperature, °C	74.7	0.5	107	0.3
Ambient temperature, °C	20.9	0.6	20.5	0.2
CO, ppm	700.1	214.1	445.2	126.4
CO, %	0.00070	0.00021	0.00045	0.00013
y, %	0.0227	0.0046	0.0475	0.0044
CO_2, %	0.0293	0.0058	0.0612	0.0056
Λ	7.19	1.38	3.36	0.29
η, %	85.82	3.00	89.74	0.78
qA, %	14.18	3.00	10.26	0.78
NO, ppm	17.9	6.7	43.2	6.0
Calculated n	6.94	1.33	3.26	0.28
X ($x = [V_{CO2}/(V_{CO2}+V_{CO})]$-n)	0.966	0.016	0.991	0.002

From these data, it can be inferred that a decrease in excess air coefficient (n) was found, total fume volume was reduced, which implies a decrease in losses due to sensitive enthalpy of fumes (q_a), increasing the yield (η). This behavior is in accordance with theory.

On the other hand, when excess air coefficient decreased, the percentage of carbon monoxide is reduced, increasing the gas ratio that is burned (x), and increasing the percentage of carbon dioxide, which implies a decrease in loss due to unburned gas, equally increasing the yield of the process (η). It should be pointed out that CO emissions from biomass combustion could be influenced by three factors: gas temperature, oxygen concentration and fuel-oxygen mixing. More oxygen would result in either a reduced gas temperature or additional residence time for a well-mixed combustion. Consequently, the design of the stove plays an important role to provide enough air during combustion process [43]. Previous studies pointed out the requirement of a suitable air supply, trying to avoid high airflow rates to reduce CO emissions [42]. This way, if x is increased, it means that combustion is more complete, decreasing the loss due to unburned gas, but it is contradictory compared to the graph yield-loss and excess air coefficient, where low values of n would imply an increase in losses due to unburned gas. Similar trends were observed with air distribution in a wood stove (with an increase in CO emissions with higher air supply ratios) [44].

Preprints (www.preprints.org) | NOT PEER-REVIEWED | Posted: 28 September 2023 doi:10.20944/preprints202309.1974.v1

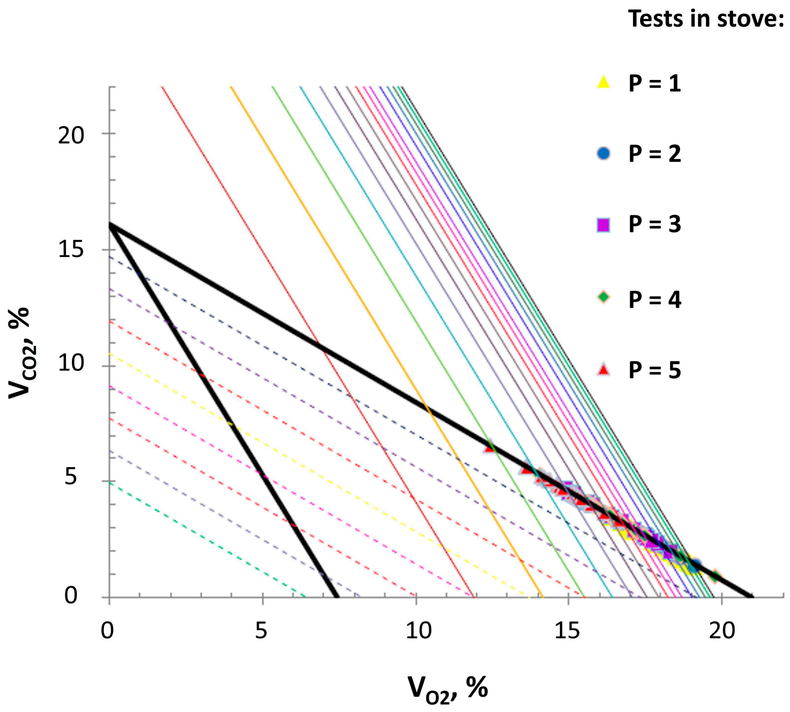

Figure 11. Ostwald diagram for pine pellets and experimental results for each level used in the combustion stove (standard feed).

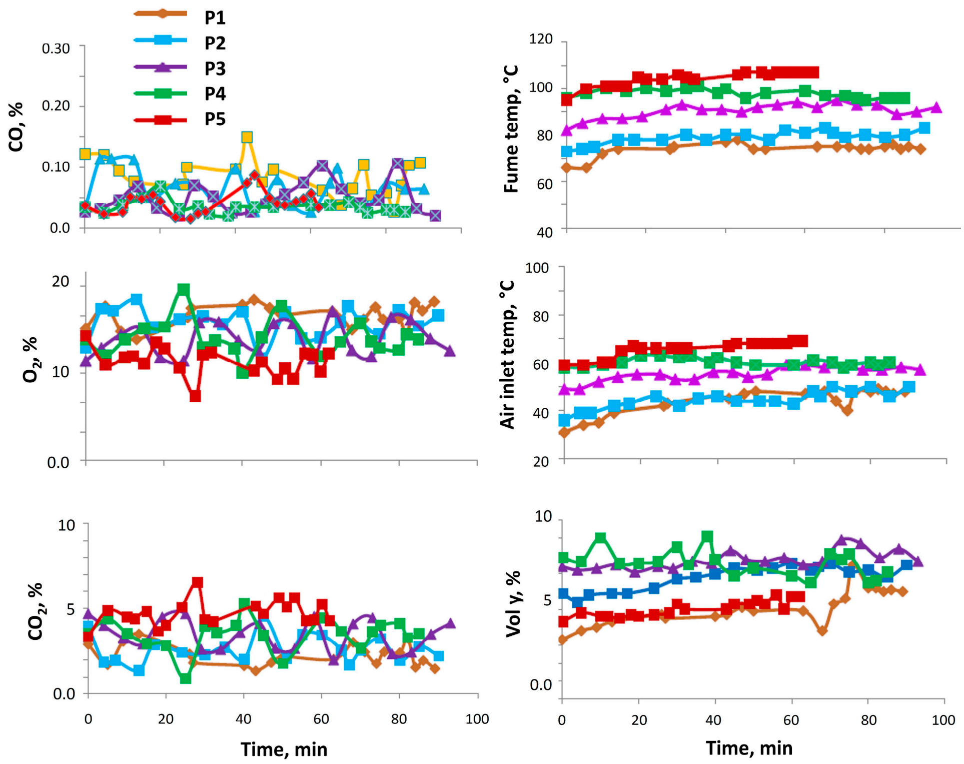

Figure 12. Evolution of main parameters for pine pellet combustion.

Concerning the outlet temperature (fume temperature, Figure 12), it considerably increased from Position 1 to Position 5, which means an increase in losses due to sensitive enthalpy, as observed in previous studies for increasing input levels or positions (from 6 to 12 kW) [34]. Consequently, the yield of the process is reduced. Nevertheless, in this case, the yield increased due to the reduction in excess air coefficient, decreasing the total volume of fumes and the losses due to sensitive enthalpy.

Preprints (www.preprints.org) | NOT PEER-REVIEWED | Posted: 28 September 2023 doi:10.20944/preprints202309.1974.v1

This way, the yield was improved. In other words, there are two opposite effects, where the decrease in fume volume is more important than the increase in fume temperature when it comes to yield determination.

Regarding room temperature, it was kept practically constant during the different experiments, whereas there was an increase in NO content with power, as observed in Table 8, even though this increase could be considered negligeable due to the low concentration of this pollutant.

Finally, inlet air temperature increased with power (Figure 12), which not necessarily implies an increase in yield, as inlet air temperature is directly related to the useful power. Thus, paying attention to the yield concept, if there is a similar air flow, an increase in inlet air temperature would mean an increase in yield, but in this case the excess air coefficient decreased. Therefore, this parameter is not determinant in yield calculations. An increase in inlet temperature is interesting if the stove working conditions are optimal.

The average deviation indicates that the measurements obtained in this work have been correctly taken, proving the homogeneity of the sampling process. Table 9 shows a comparison between different combustion conditions for pine pellets. Thus, the opposite conditions, that is, P1 with standard biomass feeding and P5 with 25 % extra feeding were compared. The abovementioned differences are clearer in this example, proving that combustion is more efficient when 25 % extra was fed. In other words, when experimental data are located on the left of the Ostwald diagram, the conditions would be more suitable for this combustion stove and using pine pellets as a fuel.

Table 9. Comparison of different levels (or positions) and feeding ratio for pine pellet (example for P=1, 100% feed and P=5, 125 % feed).

Test parameter	Pine pellet (P = 1, 100 % feed)	Pine pellet (P = 5, 125 % feed)	Comparison
O_2, %	0.18	0.119	↓
Air supply temperature, °C	46.7	90.6	↑↑↑
Fume temperature, °C	74.7	113.1	↑↑↑
Ambient temperature, °C	20.9	20.8	Constant
CO, ppm	700.1	364.4	↓↓
CO, %	0.00070	0.00036	↓↓
y, %	0.0227	0.0696	↑↑
CO_2, %	0.0293	0.0896	↑↑
Λ	7.19	2.29	↓↓↓
η, %	85.82	92.34	↑↑
qA, %	14.18	7.66	↓↓
NO, ppm	17.9	65.1	Negligible
Calculated n	6.94	2.24	↓↓
x ($x = [V_{CO2}/(V_{CO2}+V_{CO})]$-n)	0.966	0.995	↑

Regarding different feed rations when the same power was selected (in this case, P5, as observed in Figure 13), a higher increase in air inlet and fume temperatures, as well as carbon dioxide percentage, was found in the case of 125 % feed. After 30 minutes, these parameters were stabilized, as observed in the literature for similar facilities (where gas composition and energy output achieved stability after 20 minutes of ignition) [45].

Preprints (www.preprints.org) | NOT PEER-REVIEWED | Posted: 28 September 2023 doi:10.20944/preprints202309.1974.v1

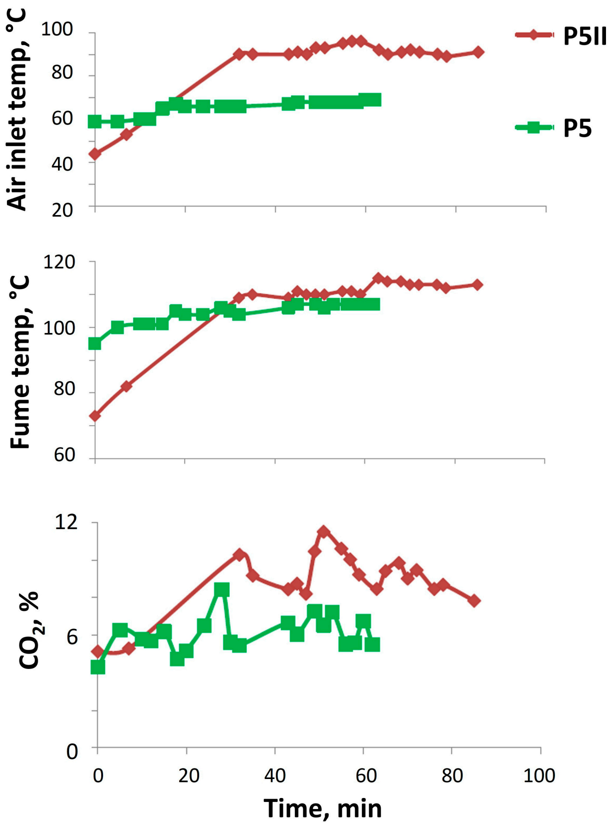

Figure 13. Comparison between different feeding rates in the case of pine pellets.

3.3. Plum Tree Pellet Combustion

Concerning plum tree pellets, the main results are included in Table 10 (where Position 2 and Position 4 were selected) and Figures 14 and 15. Similar trends were observed compared with pine pellets, except for CO emissions (see Figure 15), whose values presented a constant trend in general, as observed in previous studies during stable combustion of biomass in a commercial boiler [46].

Table 10. Comparison between P2 and P4 for plum tree combustion.

	P2		P4	
Parameter	**Average**	**Average deviation**	**Average**	**Average deviation**
O_2, %	0.189	0.004	0.180	0.007
Air supply temperature, °C	43.6	0.7	52	0.4
Fume temperature, °C	69.2	0.6	90.2	1.1
Ambient temperature, °C	18.8	0.4	18.7	0.5
CO, ppm	1378.0	240.8	1372.6	533.1
CO, %	0.00138	0.00024	0.00137	0.00053
y, %	0.0150	0.0035	0.0222	0.0057
CO_2, %	0.0198	0.0045	0.0291	0.0073
Λ	10.05	1.92	7.06	1.46
η, %	79.98	4.42	81.26	4.69
qA, %	20.02	4.42	18.74	4.69
NO, ppm	40	11.2	61.4	12.9
Calculated n	9.72	1.87	6.82	1.42
X (x = $[V_{CO2}/(V_{CO2}+V_{CO})]-n$)	0.908	0.029	0.932	0.038

Preprints (www.preprints.org) | NOT PEER-REVIEWED | Posted: 28 September 2023 doi:10.20944/preprints202309.1974.v1

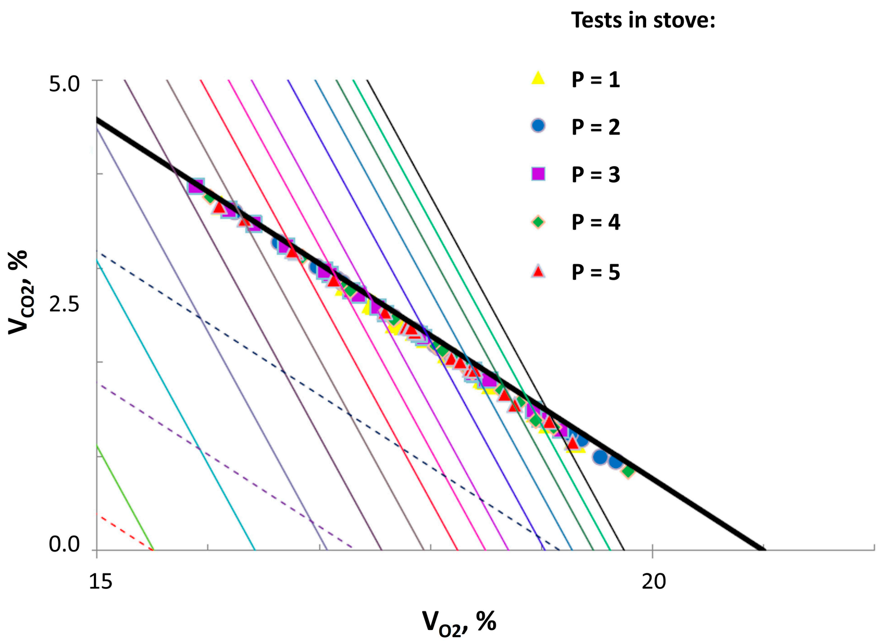

Figure 14. Ostwald diagram for plum tree pellets and experimental results for each level used in the combustion stove.

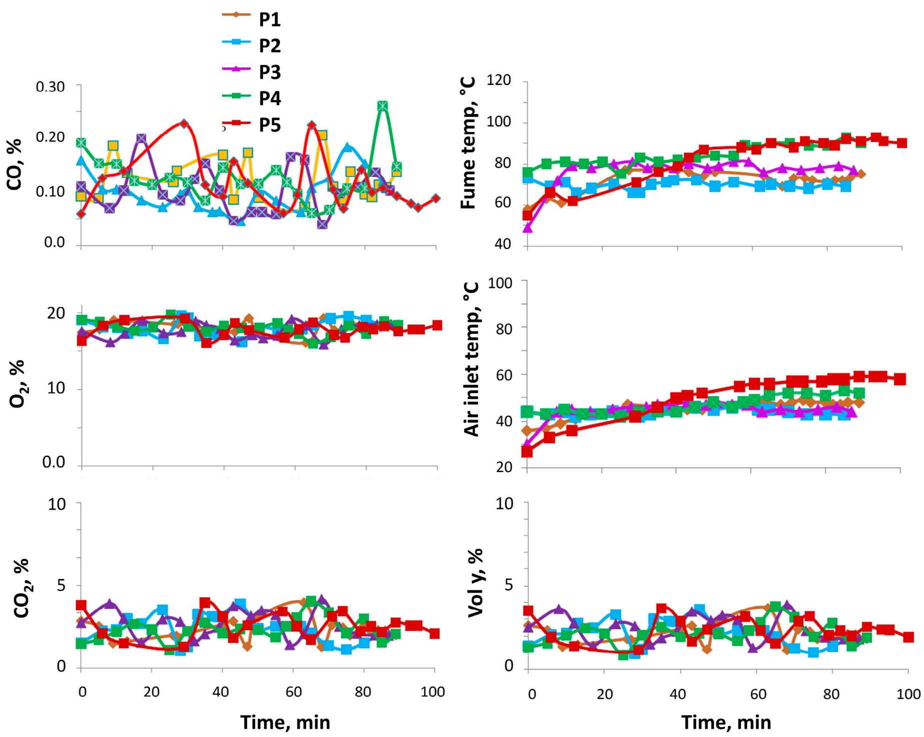

Figure 15. Evolution of main parameters for plum tree pellet combustion.

Regarding the comparison of different levels and feeding ratios for plum tree pellet, the main results are observed in Table 11. This way, when the extreme cases were compared, there were considerable differences, being in this case more noticeable with regard to the examples selected for pine pellets. Thus, it can be seen more clearly that the stove works in more optimal conditions when extra feed is selected for plum tree pellets.

Preprints (www.preprints.org) | NOT PEER-REVIEWED | Posted: 28 September 2023 doi:10.20944/preprints202309.1974.v1

Table 11. Comparison of different levels and feeding ratio for plum tree pellet (example for P=2, 100% feed and P=4, 125 % feed).

Test parameter	Plum tree pellet (P = 2, 100 % feed)	Plum tree pellet (P = 4, 125 % feed)	Comparison
O_2, %	0.189	0.141	↓
Air supply temperature, °C	43.6	49.1	↑
Fume temperature, °C	69.2	91.7	↑↑
Ambient temperature, °C	18.8	18.9	Constant
CO, ppm	1378	329.3	↓↓↓
CO, %	0.00138	0.00033	↓↓
y, %	0.0150	0.0526	↑↑
CO_2, %	0.0198	0.0671	↑↑
Λ	10.05	3.01	↓↓↓
η, %	79.98	91.53	↑↑
qA, %	20.02	8.41	↓↓
NO, ppm	40	115.9	Negligible
Calculated n	9.72	2.92	↓↓
x (x = [$V_{CO2}/(V_{CO2}+V_{CO})$]-n)	0.908	0.994	↑

In addition, when different feed rates were compared for the same level, differences with pine pellets can be found, with negligible differences in air inlet and fume temperatures, whereas CO_2 percentage was higher with 125 % feed.

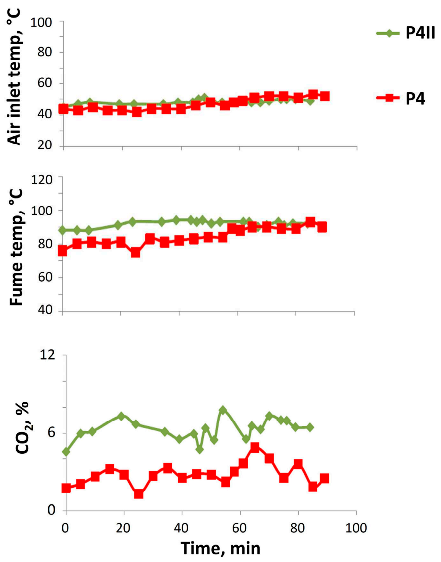

Figure 16. Comparison between different feeding rates in the case of plum tree pellets.

3.4. Poplar Pellet Combustion

Regarding Poplar pellets and their combustion performance in the domestic boiler, the main results for different powers are included in Table 12 and Figures 17 and 18. As observed, when power was increased, excess air coefficient (n) decreased. However, unlike pine and plum tree pellets, burned gas ratio (x) was kept practically constant regardless the level or position selected, increasing fume temperature and, subsequently, keeping the yield of the process constant. These results are consistent, as η did not decrease as much as in the two previous cases, not considerably decreasing fume total volume. In contrast, fume temperature increased in this case (see Figure 18). This fact could mean that loss due to sensible heat are practically constant and, considering the constant trend observed for x, this implied a constant yield throughout the experience.

 doi:10.20944/preprints202309.1974.v1

Table 12. Comparison between P3 and P5 for poplar pellet combustion.

Parameter	P3 Average	P3 Average deviation	P5 Average	P5 Average deviation
O_2, %	0.171	0.011	0.166	0.006
Air supply temperature, °C	60.7	1.0	58.8	1.1
Fume temperature, °C	78.8	1.2	96.6	1.3
Ambient temperature, °C	14.2	0.5	18.9	0.5
CO, ppm	806.7	182.4	1047.1	158.5
CO, %	0.00081	0.00018	0.00105	0.00016
y, %	0.0290	0.0085	0.0328	0.0045
CO_2, %	0.0376	0.0109	0.0426	0.0057
Λ	5.76	1.33	4.77	0.61
η, %	85.62	3.46	85.47	1.85
qA, %	14.38	3.46	14.57	1.85
NO, ppm	73.7	15.6	114.7	13.6
Calculated n	5.56	1.28	4.62	0.58
x ($x = [V_{CO2}/(V_{CO2}+V_{CO})]-n$)	0.969	0.012	0.968	0.009

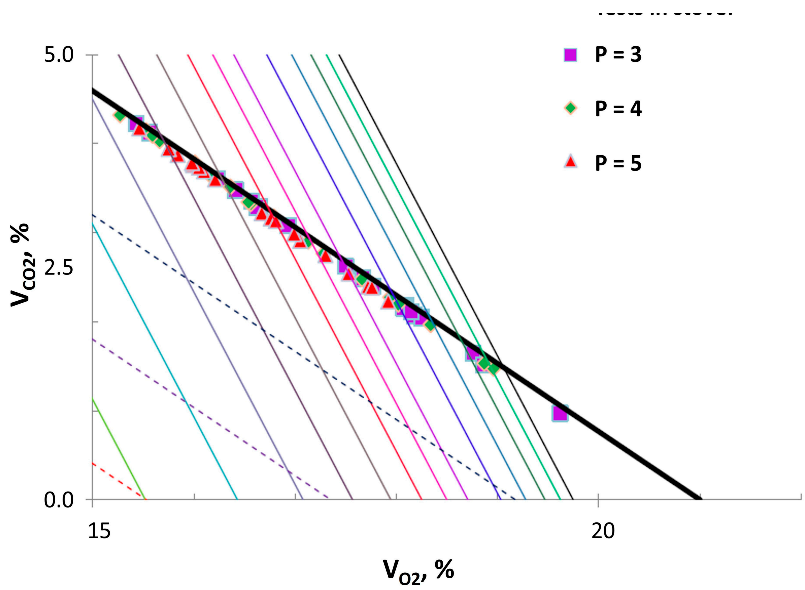

Figure 17. Ostwald diagram for poplar pellets and experimental results for each level used in the combustion stove.

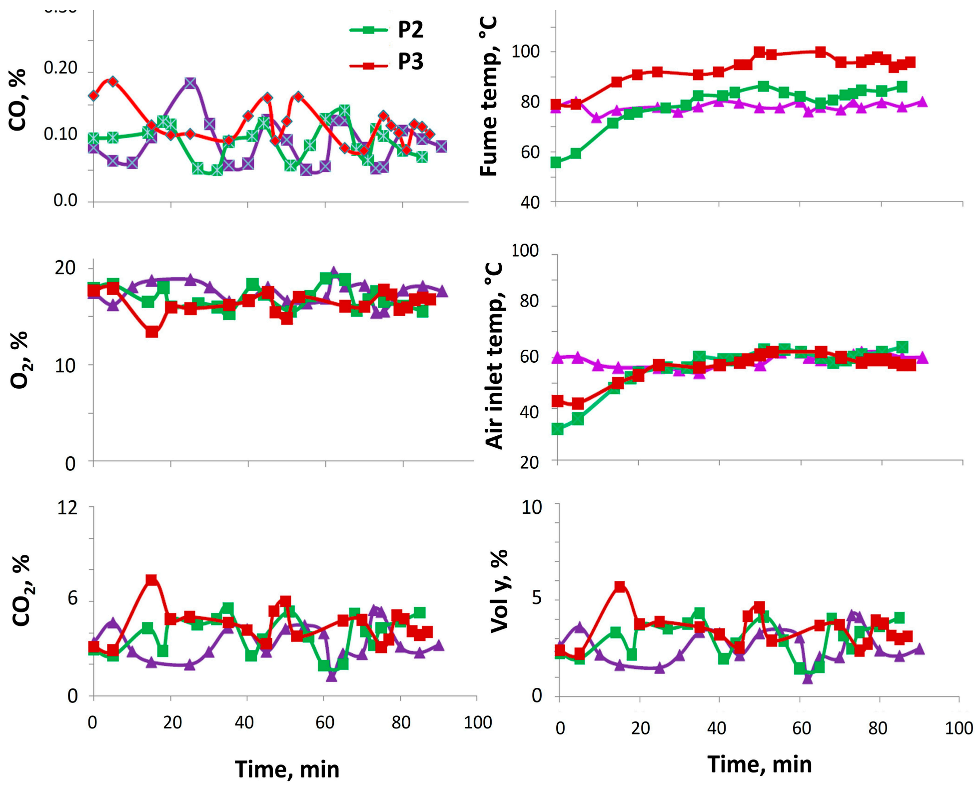

Figure 18. Evolution of main parameters for poplar pellet combustion.

When extreme conditions were compared (see Table 13), the same trends were observed as in the case of pine and plum tree pellets, concluding that a decrease in excess air implied a more optimal combustion conditions. Higher carbon dioxide emissions are related to higher temperatures in combustion processes, requiring temperature control according to previous studies where combustion emissions analysis of sugarcane bagasse were carried out in a burner pilot [47].

Table 13. Comparison of different levels and feeding ratio for poplar pellet (example for P=3, 100% feed and P=5, 125 % feed).

Test parameter	Pine pellet (P = 3, 100 % feed)	Pine pellet (P = 5, 125 % feed)	Comparison
O_2, %	0.171	0.125	↓
Air supply temperature, °C	60.7	77	↑
Fume temperature, °C	78.8	115.6	↑↑
Ambient temperature, °C	14.2	21	↑
CO, ppm	806.7	1058.6	Constant
CO, %	0.00081	0.00106	Constant
y, %	0.0290	0.0640	↑↑
CO_2, %	0.0376	0.0828	↑↑
Λ	5.76	2.45	↓↓↓
η, %	85.62	90.53	↑
qA, %	14.38	9.47	↓↓
NO, ppm	73.7	165.4	Negligible
Calculated n	5.56	2.39	↓
x ($x = [V_{CO2}/(V_{CO2}+V_{CO})]-n$)	0.969	0.984	↑

Finally, according to Figure 19, increasing the feeding rate showed similar results compared to previous pellets, although a constant CO percentage, along with a lower increase in fume temperature when pellet feed was 125 %, implied a higher yield for poplar pellet combustion. It should be noted that the behavior of different kinds of biomass could differ in certain aspects such as carbon monoxide or carbon dioxide emissions, depending on their composition and disposition (raw, briquette or pellet) [22,28,48].

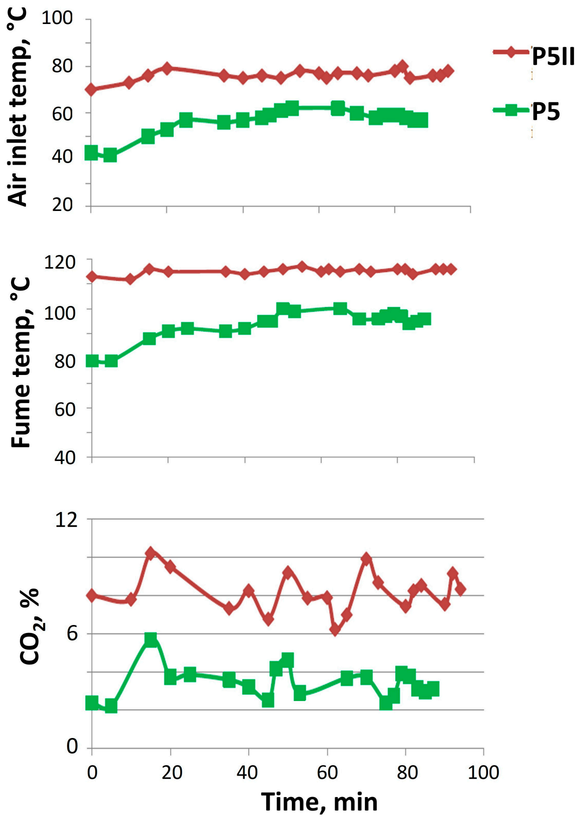

Figure 19. Comparison between different feeding rates in the case of poplar pellets.

4. Conclusions

The main findings inferred from the results of this research work were the following:

- In general, when power increased, combustion was more efficient except for poplar pellets. Also, when pellet feed flow increased, combustion was more efficient, with a special positive effect in plum tree pellets. Thus, carbon monoxide emissions were reduced, except for poplar pellets.
- Inlet air and outlet fume temperatures increased with the working level (that is, power), except for poplar pellets in the case of inlet air temperature.
- Combustion is more complete when power and feed increased, decreasing energy loss except for poplar pellets. Regarding pine and plum tree pellets, yield increased with a rise in pellet feed and power, except for poplar pellets where this yield improved by modifying excess air.
- Thus, some solutions to energy loss according to these results were proposed, such as sample homogenization to make feeding rate more stable, a reduction in excess air coefficient and the implementation of an economizer (in order to reduce fume temperature, which is a good step from environmental and economic points of view).
- In particular, the optimum combustion conditions for pine pellets were obtained by selecting Position 5 and +25 % biomass feed, with a highest yield of 92.34 % for an excess air coefficient of 2.23, a burned gas ratio of 0.994 and fumes and inlet air temperatures of 113.14 °C and 90.57 °C, respectively.
- Regarding plum tree pellets, Position 4 and +25 % biomass feed were selected for the optimum conditions in the commercial combustion stove, with a highest yield of 91.58 % for an excess air coefficient of 2.91, a burned gas ratio of 0.993 and fumes and inlet air temperatures of 91.71 °C and 49.14 °C, respectively.

- Concerning poplar pellets, optimum conditions were found when P = 3 and +25 % biomass supply were selected, with a highest yield of 91.1 % for an excess air coefficient of 3.18, and fumes and inlet air temperatures of 87.66 °C and 84.66 °C, respectively.
- To sum up, for this combustion chamber, it can be concluded that the three fuels studied are suitable for this facility in order to achieve optimum conditions, that is, an efficient combustion process, not showing considerable differences among them to be selected as an ideal biomass for this experience.

Author Contributions: Conceptualization, J.F.G. and A.A.M.; methodology, J.F.G. and A.A.M.; validation J.F.G. and A.A.M.; formal analysis, A.A.M. and D.D.C.; investigation, A.A.M. and D.D.C.; resources, J.F.G.; data curation, A.A.M. and S.N.; writing—original draft preparation, A.A.M., D.D.C. and S.N.; writing—review and editing, J.F.G. and S.N.; visualization, J.F.G., A.A.M. and S.N.; supervision, J.F.G. and A.A.M.; project administration, J.F.G.; funding acquisition, J.F.G. and A.A.M. All authors have read and agreed to the published version of the manuscript.

Funding: This research received no external funding.

Institutional Review Board Statement: Not applicable.

Informed Consent Statement: Not applicable.

Acknowledgments: The authors would like to thank CICYTEX for the raw material provided for this experience.

Conflicts of Interest: The authors declare no conflict of interest. The funders had no role in the design of the study; in the collection, analyses, or interpretation of data; in the writing of the manuscript; or in the decision to publish the results.

References

1. Högselius, P.; Kaijser, A. Energy Dependence in Historical Perspective: The Geopolitics of Smaller Nations. *Energy Policy* 2019, *127*, 438–444.
2. Vakulchuk, R.; Overland, I.; Scholten, D. Renewable Energy and Geopolitics : A Review. *Renewable and Sustainable Energy Reviews* **2020**, *122*, 109547, doi:10.1016/j.rser.2019.109547.
3. Bricout, A.; Slade, R.; Staffell, I.; Halttunen, K. From the Geopolitics of Oil and Gas to the Geopolitics of the Energy Transition: Is There a Role for European Supermajors? *Energy Res Soc Sci* 2022, *88*.
4. Scholten, D.; Bosman, R. The Geopolitics of Renewables; Exploring the Political Implications of Renewable Energy Systems. *Technol Forecast Soc Change* **2016**, *103*, 273–283, doi:10.1016/j.techfore.2015.10.014.
5. Carfora, A.; Pansini, R.V.; Scandurra, G. Energy Dependence, Renewable Energy Generation and Import Demand: Are EU Countries Resilient? *Renew Energy* **2022**, *195*, 1262–1274, doi:10.1016/j.renene.2022.06.098.
6. UN Sustainable Development Goals. **2019**.
7. Singh, A.; Christensen, T.; Panoutsou, C. Policy Review for Biomass Value Chains in the European Bioeconomy. *Glob Transit* **2021**, *3*, 13–42, doi:10.1016/j.glt.2020.11.003.
8. Vitoussia, T.; Leyssens, G.; Trouvé, G.; Brillard, A.; Kemajou, A.; Njeugna, E.; Brilhac, J.F. Analysis of the Combustion of Pellets Made with Three Cameroonian Biomass in a Domestic Pellet Stove. *Fuel* **2020**, *276*, doi:10.1016/j.fuel.2020.118105.
9. Bioenergy Europe Wood Pellet Production Worldwide from 2000 to 2018 Available online: https://www.statista.com/statistics/509075/global-wood-pellet-production/ (accessed on 18 September 2023).
10. EurObserv'ER Solid Biomass Primary Energy Production in the European Union 2000-2021 Available online: https://www.statista.com/statistics/799329/solid-biomass-energy-production-european-union-eu/ (accessed on 18 September 2023).
11. Federal Network Agency Number of Biomass Power Plants in Germany from 2011 to 2022 Available online: https://www.statista.com/statistics/457781/biomass-plants-in-germany/ (accessed on 18 September 2023).
12. Energy Information Administration Electricity Generation from Biomass and Waste in Africa from 2000 to 2020 Available online: https://www.statista.com/statistics/1276088/electricity-generation-from-biomass-and-waste-in-africa/ (accessed on 18 September 2023).

13. EurObserv'ER Biomass Energy Production and Consumption in Finland 2015-2016 Available online: https://www.statista.com/statistics/799434/solid-biomass-production-consumption-finland/ (accessed on 18 September 2023).
14. EurObserv'ER Biomass Energy Production and Consumption in Sweden 2016-2021 Available online: https://www.statista.com/statistics/799426/solid-biomass-production-consumption-sweden/ (accessed on 18 September 2023).
15. EurObserv'ER Biomass Energy Production and Consumption in Portugal 2016-2021 Available online: https://www.statista.com/statistics/799491/solid-biomass-production-consumption-portugal/ (accessed on 18 September 2023).
16. EurObserv'ER Biomass Energy Production and Consumption in Italy 2016-2018 Available online: https://www.statista.com/statistics/799429/solid-biomass-production-consumption-italy/ (accessed on 18 September 2023).
17. EurObserv'ER Biomass Energy Production and Consumption in Spain 2015-2021 Available online: https://www.statista.com/statistics/799448/solid-biomass-production-consumption-spain/ (accessed on 18 September 2023).
18. Moayedi, H.; Aghel, B.; Abdullahi, M.M.; Nguyen, H.; Safuan A Rashid, A. Applications of Rice Husk Ash as Green and Sustainable Biomass. *J Clean Prod* **2019**, *237*, 117851, doi:10.1016/j.jclepro.2019.117851.
19. Lewandowski, W.M.; Ryms, M.; Kosakowski, W. Thermal Biomass Conversion: A Review. *Processes* **2020**, *8*, doi:10.3390/PR8050516.
20. Hustad, J.E.; Wnju, O.K. *BIOMASS COMBUSTION IN II3A COUNTRES*; 1992; Vol. 2;.
21. Oladosu, K.O.; Babalola, S.A.; Kareem, M.W.; Ajimotokan, H.A.; Kolawole, M.Y.; Issa, W.A.; Olawore, A.S.; Ponle, E.A. Optimization of Fuel Briquette Made from Bi-Composite Biomass for Domestic Heating Applications. *Sci Afr* **2023**, *21*, doi:10.1016/j.sciaf.2023.e01824.
22. Pokhrel, R.P.; Gordon, J.; Fiddler, M.N.; Bililign, S. Determination of Emission Factors of Pollutants From Biomass Burning of African Fuels in Laboratory Measurements. *Journal of Geophysical Research: Atmospheres* **2021**, *126*, doi:10.1029/2021JD034731.
23. Labbé, R.; Paczkowski, S.; Knappe, V.; Russ, M.; Wöhler, M.; Pelz, S. Effect of Feedstock Particle Size Distribution and Feedstock Moisture Content on Pellet Production Efficiency, Pellet Quality, Transport and Combustion Emissions. *Fuel* **2020**, *263*, doi:10.1016/j.fuel.2019.116662.
24. Brandelet, B.; Rose, C.; Landreau, J.; Druette, L.; Rogaume, Y. Toward a Cleaner Domestic Wood Heating by the Optimization of Firewood Stoves? *J Clean Prod* **2021**, *325*, doi:10.1016/j.jclepro.2021.129338.
25. Han, J.; Liu, X.; Hu, S.; Zhang, N.; Wang, J.; Liang, B. Optimization of Decoupling Combustion Characteristics of Coal Briquettes and Biomass Pellets in Household Stoves. *Chin J Chem Eng* **2023**, doi:10.1016/j.cjche.2022.12.012.
26. Shaisundaram, V.S.; Chandrasekaran, M.; Sujith, S.; Praveen Kumar, K.J.; Shanmugam, M. Design and Analysis of Novel Biomass Stove. In Proceedings of the Materials Today: Proceedings; Elsevier Ltd, 2020; Vol. 46, pp. 4054–4058.
27. Zhang, H.; Zhang, X.; Wang, Y.; Bai, P.; Hayakawa, K.; Zhang, L.; Tang, N. Characteristics and Influencing Factors of Polycyclic Aromatic Hydrocarbons Emitted from Open Burning and Stove Burning of Biomass: A Brief Review. *Int J Environ Res Public Health* 2022, *19*.
28. Qi, J.; Liu, L.; Wu, J. Improving Combustion Technology for Cooking Activities for Pollutant Emission Reduction and Carbon Neutrality. *Atmosphere (Basel)* **2022**, *13*, doi:10.3390/atmos13040561.
29. Huang, Y.; Partha, D.B.; Harper, K.; Heyes, C. Impacts of Global Solid Biofuel Stove Emissions on Ambient Air Quality and Human Health. *Geohealth* **2021**, *5*, doi:10.1029/2020GH000362.
30. Lustenberger, D.; Strassburg, J.; Strebel, T.; Mangold, F.; Griffin, T. Simulation Tool for the Development of a Staged Combustion Pellet Stove Controller. *Energies (Basel)* **2022**, *15*, doi:10.3390/en15196969.
31. Al-Kassir, A.; Coelho, P.; García-Sanz-Calcedo, J.; Moral, F.J.; Al-Karany, R.K.; Yusaf, T. An Experimental Technology of Drying and Clean Combustion of Biomass Residues. *Applied Sciences (Switzerland)* **2018**, *8*, doi:10.3390/app8060905.
32. Maxwell, D.; Gudka, B.A.; Jones, J.M.; Williams, A. Emissions from the Combustion of Torrefied and Raw Biomass Fuels in a Domestic Heating Stove. *Fuel Processing Technology* **2020**, *199*, doi:10.1016/j.fuproc.2019.106266.

33. Prapas, J.; Baumgardner, M.E.; Marchese, A.J.; Willson, B.; DeFoort, M. Influence of Chimneys on Combustion Characteristics of Buoyantly Driven Biomass Stoves. *Energy for Sustainable Development* **2014**, *23*, 286–293, doi:10.1016/j.esd.2014.08.007.
34. Sungur, B.; Basar, C.; Kaleli, A. Multi-Objective Optimisation of the Emission Parameters and Efficiency of Pellet Stove at Different Supply Airflow Positions Based on Machine Learning Approach. *Energy* **2023**, *278*, doi:10.1016/j.energy.2023.127896.
35. Schmidt, G.; Trouvé, G.; Leyssens, G.; Schönnenbeck, C.; Genevray, P.; Cazier, F.; Dewaele, D.; Vandenbilcke, C.; Faivre, E.; Denance, Y.; et al. Wood Washing: Influence on Gaseous and Particulate Emissions during Wood Combustion in a Domestic Pellet Stove. *Fuel Processing Technology* **2018**, *174*, 104–117, doi:10.1016/j.fuproc.2018.02.020.
36. Vicente, E.D.; Duarte, M.A.; Calvo, A.I.; Nunes, T.F.; Tarelho, L.; Alves, C.A. Emission of Carbon Monoxide, Total Hydrocarbons and Particulate Matter during Wood Combustion in a Stove Operating under Distinct Conditions. *Fuel Processing Technology* **2015**, *131*, 182–192, doi:10.1016/j.fuproc.2014.11.021.
37. Toscano, G.; Duca, D.; Amato, A.; Pizzi, A. Emission from Realistic Utilization of Wood Pellet Stove. *Energy* **2014**, *68*, 644–650, doi:10.1016/j.energy.2014.01.108.
38. UNE Normalización Española. Solid Mineral Fuels. Determination of Ash.
39. UNE Normalización Española. Hard Coal and Anthracite. Determination of Total Moisture.
40. UNE Normalización Española. Hard Coal and Coke. Determination of Volatile Matter Content.
41. Yao, W.; Zhao, Y.; Chen, R.; Wang, M.; Song, W.; Yu, D. Emissions of Toxic Substances from Biomass Burning: A Review of Methods and Technical Influencing Factors. *Processes* 2023, *11*.
42. Deng, M.; Li, P.; Shan, M.; Yang, X. Optimizing Supply Airflow and Its Distribution between Primary and Secondary Air in a Forced-Draft Biomass Pellet Stove. *Environ Res* **2020**, *184*, doi:10.1016/j.envres.2020.109301.
43. Zhang, Y.; Zhang, Z.; Zhou, Y.; Dong, R. The Influences of Various Testing Conditions on the Evaluation of Household Biomass Pellet Fuel Combustion. *Energies (Basel)* 2018, *11*.
44. Holubčík, M.; Čajová Kantová, N.; Jandačka, J.; Čaja, A. The Performance and Emission Parameters Based on the Redistribution of the Amount of Combustion Air of the Wood Stove. *Processes* **2022**, *10*, doi:10.3390/pr10081570.
45. Wang, X.; Niu, B.; Deng, S.; Liu, Y.; Tan, H. Optimization Study on Air Distribution of an Actual Agriculture Up-Draft Biomass Gasification Stove. In Proceedings of the Energy Procedia; Elsevier Ltd, 2014; Vol. 61, pp. 2335–2338.
46. Lasek, J.A.; Matuszek, K.; Hrycko, P.; Głód, K.; Li, Y.H. The Combustion of Torrefied Biomass in Commercial-Scale Domestic Boilers. *Renew Energy* **2023**, *216*, doi:10.1016/j.renene.2023.119065.
47. Costa, M.A.M.; Schiavon, N.C.B.; Felizardo, M.P.; Souza, A.J.D.; Dussán, K.J. Emission Analysis of Sugarcane Bagasse Combustion in a Burner Pilot. *Sustain Chem Pharm* **2023**, *32*, doi:10.1016/j.scp.2023.101028.
48. Kougioumtzis, M.A.; Kanaveli, I.P.; Karampinis, E.; Grammelis, P.; Kakaras, E. Combustion of Olive Tree Pruning Pellets versus Sunflower Husk Pellets at Industrial Boiler. Monitoring of Emissions and Combustion Efficiency. *Renew Energy* **2021**, *171*, 516–525, doi:10.1016/j.renene.2021.02.118.